WARSAW UNIVERSITY OF TECHNOLOGY Index 351733
FACULTY OF CIVIL ENGINEERING
COMMITTEE FOR CIVIL AND WATER ENGINEERING
POLISH ACADEMY OF SCIENCES ISSN 1230-2945

DOI: 10.24425/ace.2026.157467

ARCHIVES OF CIVIL ENGINEERING

Vol. LXXII ISSUE 1 2026

pp. 169–184

Research paper

Research on the mechanism of graphene/rubber composite-modified asphalt based on molecular dynamics

Shaobo Huo[1], Bo Chen[2], Yu Lei[3]

Abstract: To study the modification mechanism of graphene/rubber composite-modified asphalt, the blending system of graphene, rubber, and asphalt was studied by molecular dynamics simulation. The molecular models of asphalt, rubber asphalt, and graphene/rubber composite-modified asphalt were constructed by molecular dynamics software. The intermolecular binding energy, radial distribution function, and mechanical properties of the three asphalt systems were studied. The results showed that the addition of graphene increased the binding energy between rubber and light components of asphalt, promoted the absorption of light components of rubber, improved the binding stability of rubber and resin, and improved the compatibility of rubber and asphalt. Graphene can weaken the agglomeration behavior of asphaltene and rubber, and promote light components to penetrate and fill the agglomeration space between asphaltene, which improves the overall stability of the asphaltene system. Graphene promoted the swelling development of rubber and made rubber form a stable spatial grid structure in the asphalt, thus contributing to the elastic modulus, bulk modulus, and shear modulus of graphene/rubber and asphalt blending system compared to the matrix asphalt has a greater enhancement.

Keywords: graphene, molecular dynamics, modified asphalt, modification mechanism

[1]Eng., CCCC-SHEC Engineering Testing Technology Co. Ltd., Xi'an, 710065, China, e-mail: 18435368536@163.com, ORCID: 0009-0002-1130-9364
[2]Eng., CCCC-SHEC Engineering Testing Technology Co. Ltd., Xi'an, 710065, China, e-mail: 931264973@qq.com, ORCID: 0009-0008-5675-6698
[3]Eng., CCCC Second Highway Engineering Co., Ltd., Xi'an, 710065, China, e-mail: 794868984@qq.com, ORCID: 0000-0001-9836-351X

1. Introduction

Rubber, as a high-performance modifier, not only improves the performance of asphalt and asphalt mixtures and extends the life of asphalt pavements, but also contributes to substantial cost savings, environmental protection, and integrates road construction into the framework of sustainable development [1]. Meanwhile, nanomaterials have also attracted much attention due to nanoscale phenomena such as high surface energy and quantum size effect [2–4]. Graphene is a honeycomb carbon nanomaterial formed by the hybridization of C atoms through sp^2 orbitals [5, 6]. Once produced, it has attracted the attention of many researchers due to its excellent high strength and high toughness. Road workers compounded graphene and rubber-modified asphalt and found that the performance of asphalt has been significantly improved. For example, Meng et al. [7] conducted frequency scanning tests on graphene/rubber composite modified asphalt and found that graphene could improve the high temperature performance of asphalt. Zou et al. [8] conducted rheological tests at high and low temperatures on graphene rubber asphalt, and the results showed that the high temperature stability and low temperature crack resistance of asphalt were significantly improved. However, these scholars characterized the impact of graphene and rubber on asphalt properties through macroscopic experimental means, but did not fundamentally explain why graphene and rubber can comprehensively and thoroughly improve the performance of asphalt. Therefore, it is necessary to find a new method to reveal the modification mechanism of graphene and rubber on asphalt.

Molecular dynamics (MD) originated in physics and is widely used in different research fields [9]. It is a computational method based on statistical mechanics and thermodynamics theory, used to simulate the interactions and behaviors of atoms and molecules under certain conditions. Meanwhile, the chemical-physical properties and thermodynamic properties of molecular systems can be obtained after simulation [10]. Therefore, molecular dynamics simulation is an excellent tool for quantitatively characterizing the microscopic state of materials and a new method for exploring the relationship between the macroscopic performance and microscopic mechanisms of materials [11]. In recent years, with the improvement of computer hardware, molecular dynamics has been gradually applied by researchers in the field of road materials. It uses particle-based molecular interactions and local dynamic analysis to study the main physical and mechanical properties of asphalt materials. It has been widely applied to calculate the main characteristics of asphalt, including density, glass transition temperature, diffusion coefficient, adhesion, and self-healing behavior [12]. Liu et al [13] investigated the activation mechanism of a rejuvenation agent in recycled asphalt pavement binder by using MD simulation, and the results showed that the addition of a rejuvenation agent increased the activity of asphaltenes and resins, thus improved the bonding energy between old and new asphalt. Wei et al [14] constructed an asphalt-water-aggregate interface model and investigated the effect of moisture on the adhesion energy at the asphalt-aggregate interface. Kang et al [15] simulated the liquid-liquid transition and the glass transition of asphalt by MD, which helped to improve the understanding of the process of vitrification formation of asphalt materials

in the real environment. Pan et al [16] investigated the combined effects of oxidation and moisture on asphalt binder in the form of energy and density changes by MD simulation and found that the moisture-induced oxidized asphalt binder is the most susceptible to damage. Yaphary et al [17] investigated the nanoscale crack propagation characteristics at the interface of old and new asphalt binders in recycled asphalt mixtures by MD simulation. It was shown that at low temperatures, greater tensile stresses are generated at the mixed binders and their interfaces with the new and aged binders, and thus the interfacial crack propagation becomes more severe. Mehdi et al [18] carried out a study on the effect of rejuvenating agents on the thermo-mechanical properties of oxidized asphalt by using MD simulation, and the results showed that the amide groups in the bio-rejuvenating agents interacted with asphaltene molecules, increasing the stacking of the asphaltene dimer distance and also changed their conformational stacking, which led to the recovery of the thermo-mechanical properties of oxidized asphalt. It can be seen that molecular dynamics simulation has become a powerful tool for describing the behavior of materials and characterizing the relationship between their chemical structure and engineering properties [19].

Therefore, to reveal the modification mechanism of graphene/rubber composite-modified asphalt, this paper constructed molecular models of matrix asphalt, rubber asphalt, and graphene/rubber asphalt using the molecular dynamics software Materials Studio (MS), and explored and studied the mechanism of graphene/rubber composite-modified asphalt by the changes of radial distribution function, intermolecular binding energy, and mechanical properties.

2. Model construction and simulation methods

2.1. Establishment of matrix asphalt and modified asphalt model

According to statistics, there are 10^6 kinds of components in asphalt, and China generally divides the components of road asphalt into four kinds, respectively, asphaltene, resin, saturated, and aromatic. Therefore, a four-component asphalt molecular model was established in this paper. The research results of ($C_{53}H_{55}NOS$) were used as the asphaltene molecular model [20], benzo diisobenzothiophene ($C_{18}H_{10}S_2$) was used as the resin representative molecular model [21], *n*-docosadiane ($C_{22}H_{46}$) was used as the saturation representative molecular model, and 1,7-dimethylnaphthalene ($C_{12}H_{12}$) as an aromatic component representative molecular model [22]. For the rubber molecular model, natural rubber (NR) was used as the representative molecular model, and the repeating unit was cis-1, 4 polyisoprene. Since its molecular weight varied with the degree ofTab polymerization, the polymerization degree of natural rubber was chosen to be 12 to reduce the molecular dynamics simulation calculation time [23]. The representative molecular model of graphene was obtained by cracking graphite [24]. Finally, the software MS was used to construct each molecular model, as shown in Fig. 1.

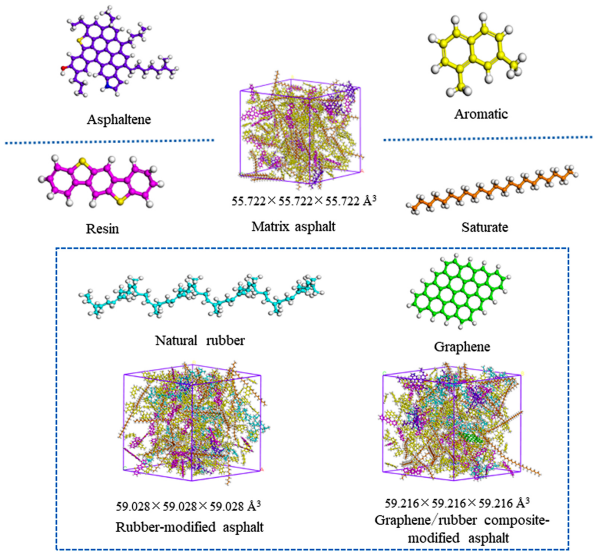

Fig. 1. Asphalt molecular model

According to the mass fraction ratio of each component in SK-90# asphalt [25], the Amorphous Cell module in MS software is used to build the molecular model of asphalt, with the initial density of 0.5 g/cm^3. In this paper, 18.24% rubber content and 0.3% graphene content were selected, and rubber asphalt molecular models and graphene/rubber composite-modified asphalt molecular models were constructed in the same steps as above, as shown in Fig. 1. The specific parameters of each component of the three asphalt models are shown in Table 1.

Table 1. Related parameters of each molecular model

Component	Chemical formula	Molar mass	Mass fraction (%)	Test result (%)
Asphaltene	$C_{53}H_{55}NOS$	754.089	7.2	7.25
Resin	$C_{18}S_2$	280.312	20.9	20.74
Saturate	$C_{22}H_{46}$	310.610	22.6	22.54
Aromatic	$C_{12}H_{12}$	156.228	49.3	49.47
Natural rubber	$C_{69}H_{98}$	819.444	18.0	18.24
Graphene	$C_{48}H_{18}$	594.672	0.4	0.3

It is worth pointing out that after the construction of each molecular model was completed, energy must be minimized to eliminate bad contacts between atoms. First, Geometry Optimization with a maximum number of iterations of 10,000 was performed on each molecular system. Then run the Anneal program in the Forcite module to perform 5 cycles of annealing treatment on the system, the temperature was set to 300–500 K, the temperature interval was 20 K, and the total annealing time was 10 ps. Next, perform a 100 ps dynamic simulation of the annealing system. The system ensemble was NVT, the accuracy was Ultra-fine, the force

field was COMPASS, the temperature was set to 298 K, the electrostatic interaction was Ewald, the van der Waals interaction was Atom based, and the cut-off distance Set to 18.5 Å. After the dynamics, the system basically reaches a steady state, and then takes the last frame to perform a 200 ps dynamic simulation under the NPT ensemble (one frame is output every 1000 steps), the temperature uses the Nose thermostat, the pressure selects the Berendsen barostat, and the pressure is set to 1 atmosphere (0.0001 GPa).

2.2. Model verification

2.2.1. Glass transition temperature

The glass transition temperature of asphalt is the characteristic temperature of asphalt from viscoelastic to glassy state, and is an important parameter in determining the viscoelastic properties of asphalt materials [26]. Therefore, the molecular dynamics simulation of matrix asphalt, rubber-modified asphalt, and graphene/rubber composite-modified asphalt was carried out under the NPT system synthesis, and the temperatures were selected to be 100 K, 150 K, 200 K, 250 K, 300 K, 350 K, 400 K, and 450 K for eight temperature points, to calculate the volume of asphalt systems at different temperatures, from which the change curves of the volume of the three asphalt systems with the temperature can be obtained as shown in Fig. 2.

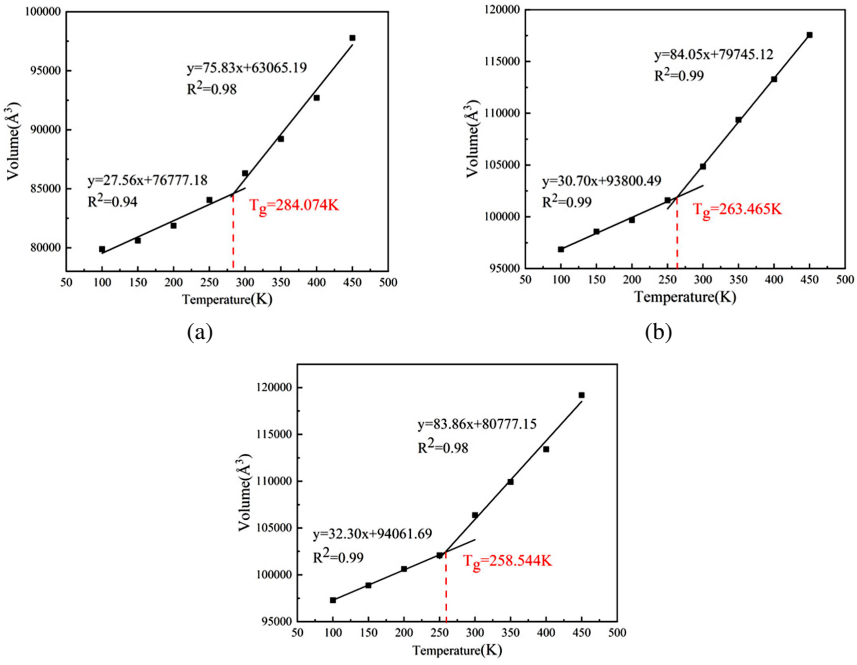

Fig. 2. Asphalt Model Volume-Temperature Curve: (a) Matrix asphalt; (b) Rubber-modified asphalt; (c) Temperature (K)

The glass transition temperature of asphalt is the intersection point of fitted linear regression line on both sides of the inflection point of asphalt volume-temperature curve. As can be seen from Fig. 2, T_g of matrix asphalt, rubber-modified asphalt and graphene/rubber composite-modified asphalt are 284.074 K, 263.465 K, and 258.544 K, respectively. The T_g value of asphalt simulation is slightly higher than the known test value, which is caused by the rapid cooling rate in the molecular simulation process, but the simulation results in this paper are still within the permissible range of the temperature change of T_g and close to the predicted results of other researchers [27, 28]. At the same time, T_g of rubber-modified asphalt and graphene/rubber composite-modified asphalt is lower than that of matrix asphalt, indicating that both rubber and graphene can improve the low temperature properties of asphalt, which is also consistent with the results obtained by scholars through BBR test [29, 30]. Therefore, the asphalt model in this study can be verified by the glass transition temperature T_g.

2.2.2. Density

Density is a direct measure to evaluate whether the model size and force field can produce accurate and reasonable simulation results, and it is the most frequently adopted parameter for asphalt model validation. In view of this, the density of the three asphalt systems was calculated at the temperature of 298 K, and the results are shown in Fig. 3.

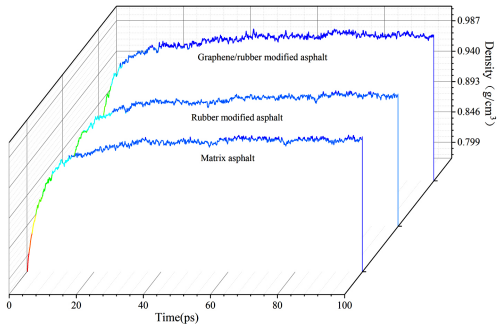

Fig. 3. Density curve of different systems with time at 298 K

It can be seen from Fig. 3 that the density of the three asphalt systems increases sharply with the increase of simulation time and becomes stable after 25 ps. However, the density values of the three asphalt systems were finally stabilized at 0.97–1.0 g/cm^3, which is close to the experimentally measured asphalt density of 1.02 ± 0.2 g/cm^3 [31]. Therefore, the density further proves that the modeling of the three asphalt systems is reliable and reasonable.

3. Results and discussion

3.1. Binding energy between components

Binding energy refers to the work that needs to be done on a system made up of multiple substances if the components are separated to “infinity”. The greater the binding energy, the more closely the system is combined, and the more stable the system. The calculation formula

of binding energy is shown in Eq. (3.1).

$$E_{\text{binding energy}} = E_A + E_B - E_{AB} \tag{3.1}$$

where: $E_{\text{binding energy}}$ – binding energy, E_A – energy of substance A, E_B – energy of substance B, E_{AB} – total energy of AB system.

The binding energy of matrix asphalt, rubber-modified asphalt, and graphene/rubber composite-modified asphalt are shown in Table 2–4.

Table 2. Binding energy between components of matrix asphalt

	Bind Energy (kcal/mol)	**Hydrogen bond**	**van der Waals**	**Electrostatic**	**Long range correction**
Asphaltene-resin	84.622	0	83.041	0.121	1.46
Asphaltene-saturate	124.769	0	122.009	0.589	2.171
Asphaltene- aromatic	320.503	0	302.558	13.459	4.486

Table 3. Binding energy between components of rubber-modified asphalt

	Bind Energy (kcal/mol)	**Hydrogen bond**	**van der Waals**	**Electrostatic**	**Long range correction**
Asphaltene-resin	116.071	0	114.994	–0.101	1.178
Asphaltene-saturate	88.129	0	86.393	–0.015	1.751
Asphaltene-aromatic	219.896	0	206.561	9.717	3.618
Rubber-asphaltene	118.545	0	116.156	0.672	1.717
Rubber-resin	58.238	0	56.152	0.394	1.692
Rubber-saturate	390.405	0	383.921	0.573	5.911
Rubber-aromatic	780.866	0	763.956	7.699	9.211

Table 4. Binding energy between components of graphene/rubber composite-modified asphalt

	Bind Energy (kcal/mol)	**Hydrogen bond**	**van der Waals**	**Electrostatic**	**Long range correction**
Asphaltene-resin	133.056	0	132.116	–0.222	1.162
Asphaltene-saturate	90.023	0	87.706	0.59	1.727
Asphaltene- aromatic	217.925	0	206.009	8.346	3.57
Rubber-asphaltene	205.292	0	201.33	–0.013	3.975
Rubber-resin	76.829	0	72.769	0.03	4.03
Rubber-saturate	428.204	0	421.63	0.583	5.991
Rubber-aromatic	809.465	0	786.248	10.838	12.379

As can be seen from Table 2, the binding energy of asphaltene with resin, saturated fraction, and aromatic fraction are all positive, indicating that the asphaltene and the components of the mutual attraction. Among them, asphaltene and aromatic components of the binding energy is the largest, and the smallest binding energy with the resin, indicating that the matrix asphaltene and aromatic components of asphaltene combination is the most stable, and the most unstable combination with the resin, that is, the asphaltene colloidal structure is not stable.

In rubber-modified asphalt, the binding energy between asphaltenes and other components is lower than that of matrix asphalt. This is because the molecular weight of aromatic and saturated molecules in asphalt is small and the molecular movement rate is relatively fast under the same conditions. After the addition of rubber to the asphalt, some of the aromatic and saturated molecules will depart from the asphaltene and move around the rubber, and rubber will compete with asphaltene for the light components in asphalt. The binding energy between asphaltene and resin increased, indicating that the addition of rubber made the colloidal structure of asphalt with asphaltene as the core and resin adsorbed on the surface more stable, and the high-temperature performance of rubber asphalt improved. At the same time, the binding energy between the rubber and the asphalt four components was also considered. The binding energy between rubber and asphalt four components is rubber-aromatic component < rubber-saturated component < rubber-asphalt component < rubber-resin component. The binding energy between rubber and resin is much smaller than that between rubber and asphaltene, saturated component, and aromatic component, which indicates that the interaction between rubber and resin is very weak and the binding is very unstable. The main reason is that the side chain length of asphaltene, saturated component, and aromatic component is different, the resin molecule is a ring structure without side chain, and the rubber molecule is also a chain structure, which makes the rubber and asphalt, saturated and aromatic side chain entangled together, increasing the binding energy between molecules. The addition of rubber will absorb some of the light components in the matrix asphalt, so that the content of freely moving light components in the asphalt is reduced. The change of asphalt from sol-colloid structure to gel-colloid structure increases the elasticity and viscosity of asphalt, decreases the temperature sensitivity, decreases the fluidity and plasticity, and improves the high temperature stability. At the same time, the combination of rubber and resin is very unstable, the molecular weight and polarity of rubber are very different from asphalt. Therefore, the storage stability of rubber asphalt is poor, easy to produce segregation.

As can be seen from Table 4 the binding energy between the components in the graphene/rubber composite-modified asphalt are all contributed by van der Waals force and electrostatic attraction, while the hydrogen bond is zero, indicating that graphene/rubber composite-modified asphalt is mainly physical modification, which is also consistent with the results of FTIR test by previous scholars [32]. The addition of graphene increases the binding energy between asphaltene and resin and saturated components, which means that the colloidal structure of asphalt becomes more stable and prevents the occurrence of asphaltene flocculation

in asphalt. At the same time, the binding energy between rubber and resin, saturated component and aromatic component increased, and the binding energy between rubber and resin increased from 58.238 kcal/mol to 76.829 kcal/mol, indicating that graphene promoted the absorption of light components in rubber, and also improved the binding stability of rubber and resin. This process enabled rubber to fully swell and develop, and uniformly dispersed in asphalt to form a multi empty three-dimensional structure, while other components would fill this multi empty three-dimensional space and combine more closely with rubber, to achieve the purpose of improving the high and low temperature performance of asphalt.

3.2. Radial distribution function

To further analyze the modification mechanism of graphene/rubber composite-modified asphalt, the radial distribution function was used to analyze the agglomeration behavior of the four components in matrix asphalt, rubber asphalt, and graphene/rubber composite-modified asphalt. The radial distribution function $g(r)$ gives the probability of occurrence of a particle at a certain distance from another particle. The calculation formula is shown in Eq. (3.2).

$$g(r) = \frac{\mathrm{d}N}{4\rho\pi r^2 \mathrm{d}r} \tag{3.2}$$

where: r – distance between particles, ρ – average density of the system, N – number of particles.

For amorphous polymers, when r is very large, $g(r)$ is equal to 1, indicating that the remote distribution of particles is disordered. When r is small, $g(r)$ will have a peak, indicating that there is a higher probability of another particle at this location. Therefore, the radial distribution function can be used to analyze molecular agglomeration in polymer models. When the peak value at one r of the radial distribution function curve is significantly higher than other places, an agglomeration structure appears between the molecules at this distance [33]. The radial distribution function among components in asphalt is shown in Fig. 4.

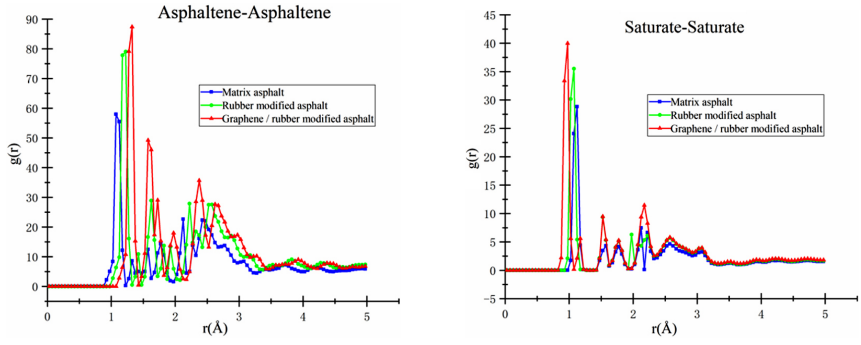

(a) (b)

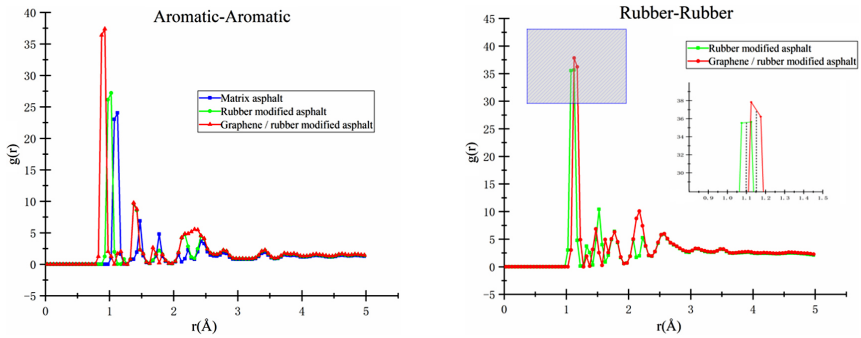

Fig. 4. Radial distribution function diagram of components in different systems: (a) Asphaltene-asphaltene; (b) Saturated-saturated; (c) Aromatic-aromatic; (d) Rubber-rubber

Figure 4(a) shows the radial distribution function of the asphaltenes, and it can be seen that the first peak appears obviously in the three kinds of asphalt. The first peak of matrix asphalt appeared at 1.075 Å, while the first peaks of rubber asphalt and graphene/rubber composite-modified asphalt appeared at 1.225 Å and 1.325 Å, indicating that the addition of rubber and graphene increased the distance between asphaltene and asphaltene to different degrees, and reduced the aggregation of asphaltene molecules.

Figures 4(b) and 4(c) are the radial distribution function diagrams between saturated-saturated and aromatic-aromatic components. In the three asphalts, the first peak of the saturated component is 1.125 Å, 1.075 Å and 0.975 Å respectively, and the first peak of the aromatic component is 1.125 Å, 1.025 Å and 0.925 Å respectively, indicating that the addition of graphene and rubber reduces the distance between saturated and aromatic components, and intensifies the agglomeration behavior of saturated components and aromatic components. At the same time, the addition of rubber and graphene also increases the peak intensity of the first peak of saturated components by 23.24% and 38.70%, and the first peak intensity of aromatic components by 13.12% and55.42%, which is due to the fact that graphene promoted the swelling development of rubber, resulting in the accumulation of saturated fraction and aromatic fraction around rubber.

Figure 4(d) shows the radial distribution function of the rubber molecules, from which it can be seen that the first peak of the rubber molecules in graphene/rubber composite-modified asphalt appeared in a relatively backward position, indicating that the addition of graphene makes the distance between rubber molecules larger, which is consistent with the results obtained by previous scholars through fluorescence image analysis [32].

In short, the addition of graphene and rubber weakens the agglomeration behavior of asphaltene molecules, and strengthens the agglomeration behavior of saturated components and aromatic components. The increase in the distance between asphaltene molecules means that more small molecules can penetrate and fill the agglomeration space between asphaltenes. The molecules in the asphalt are more tightly combined and have better stability. At the same time, it also drives the transformation of the asphalt colloid structure, and finally improves the high and low temperature performance of matrix asphalt.

3.3. Mechanical modulus

Mechanical properties are important properties of materials to resist deformation under the action of external forces, and are closely related to the preparation, processing, production, and application of materials [34]. In molecular dynamics, the methods of calculating mechanical properties include constant strain method, stress fluctuation method, and static method. The constant strain method has the shortest calculation time, but it requires high requirements for the optimization process of the structure. In this paper, the elastic stiffness matrix and elastic flexibility matrix of the three asphalt models were obtained by the conjugate gradient method, and the shear modulus and bulk modulus were calculated using the Hill method. The maximum strain was set to 0.01, and the number of steps for each strain was set to 6.The energy convergence criterion was set to 1.0×10^{-4} kcal/mol. As a result, the elastic stiffness matrix C_A (GPa) and elastic flexibility matrix S_A (TPa^{-1}) of the matrix asphalt, the elastic stiffness matrix C_R (GPa) and elastic flexibility matrix S_R (TPa^{-1}) of the rubber modified asphalt, and the elastic stiffness matrix C_G (GPa) and elastic flexibility matrix S_G (TPa^{-1}) of the graphene/rubber composite modified asphalt can be obtained as follows.

$$C_A = \begin{bmatrix} 1.5529 & 1.0697 & 0.8796 & -0.0727 & 0.0856 & -0.0076 \\ 1.0697 & 1.5370 & 0.8414 & -0.0230 & 0.1636 & 0.1354 \\ 0.8796 & 0.8414 & 1.1860 & -0.0224 & 0.1850 & -0.0413 \\ -0.0727 & -0.0230 & -0.0224 & 0.2757 & 0.1214 & 0.0867 \\ 0.0856 & 0.1636 & 0.1850 & 0.1214 & 0.2099 & -0.0192 \\ -0.0076 & 0.1354 & -0.0413 & 0.0867 & -0.0192 & 0.2651 \end{bmatrix}$$

$$S_A = \begin{bmatrix} 1550.5491 & -852.2868 & -653.5678 & -218.2427 & 780.5642 & 505.9003 \\ -852.2868 & 1756.2705 & -450.1546 & 864.2668 & -1249.4639 & -1364.7976 \\ -653.5678 & -450.1546 & 1853.5772 & 385.0399 & -1212.7568 & 286.2778 \\ -218.2427 & 864.2668 & 385.0399 & 6914.1726 & -5200.3909 & -3025.5084 \\ 780.5642 & -1249.4639 & -1212.7568 & -5200.3909 & 9761.0746 & 2879.7549 \\ 505.9003 & -1364.7976 & 286.2778 & -3025.5084 & 2879.7549 & 5726.8843 \end{bmatrix}$$

$$C_R = \begin{bmatrix} 1.4951 & 1.1929 & 0.9126 & -0.1547 & 0.0234 & 0.0280 \\ 1.1929 & 1.9455 & 0.7418 & -0.0974 & 0.0309 & -0.0330 \\ 0.9126 & 0.7418 & 1.8177 & -0.2433 & 0.2196 & 0.0937 \\ -0.1547 & -0.0974 & -0.2433 & 0.3571 & -0.0838 & 0.0174 \\ 0.0234 & 0.0309 & 0.2196 & -0.0838 & 0.3025 & 0.0081 \\ 0.0280 & -0.0330 & 0.0937 & 0.0174 & 0.0081 & 0.3716 \end{bmatrix}$$

$$S_R = \begin{bmatrix} 1645.8726 & -812.1276 & -505.0887 & 243.7362 & 392.2073 & -88.7398 \\ -812.1276 & 1019.4950 & -24.7275 & -112.4439 & -58.9217 & 164.5147 \\ -505.0887 & -24.7275 & 928.8957 & 288.5993 & -547.4320 & -199.9421 \\ 243.7362 & -112.4439 & 288.5993 & 3246.8158 & 689.7526 & -268.1879 \\ 392.2073 & -58.9217 & -547.4320 & 689.7526 & 3870.3107 & -13.4097 \\ -88.7398 & 164.5147 & -199.9421 & -268.1879 & -13.4097 & 2775.6280 \end{bmatrix}$$

$$C_G = \begin{bmatrix} 1.9102 & 1.3791 & 0.9471 & -0.0320 & 0.0053 & -0.0788 \\ 1.3791 & 2.0606 & 1.0974 & -0.0205 & -0.0366 & -0.0239 \\ 0.9471 & 1.0974 & 1.4571 & -0.1053 & -0.0639 & -0.0891 \\ -0.0320 & -0.0205 & -0.1053 & 0.4091 & -0.0381 & -0.0161 \\ 0.0053 & -0.0366 & -0.0639 & -0.0381 & 0.3905 & 0.0623 \\ -0.0788 & -0.0239 & -0.0891 & -0.0161 & 0.0623 & 0.2847 \end{bmatrix}$$

$$S_G = \begin{bmatrix} 1084.9630 & -590.1826 & -255.9860 & -16.2799 & -145.7290 & 201.6158 \\ -590.1826 & 1142.3235 & -497.6318 & -120.7629 & 60.8080 & -243.1733 \\ -255.9860 & -497.6318 & 1272.8165 & 307.2379 & 151.9394 & 269.5560 \\ -16.2799 & -120.7629 & 307.2379 & 2546.9150 & 260.9651 & 168.3180 \\ -145.7290 & 60.8080 & 151.9394 & 260.9651 & 2709.2826 & -566.0460 \\ 201.6158 & -243.1733 & 269.5560 & 168.3180 & -566.0460 & 3765.1618 \end{bmatrix}$$

According to the elastic stiffness matrix and elastic flexibility matrix, the bulk modulus K and shear modulus G of each system are calculated using the Hill method [35]. Specifically:

$$K_H = \frac{(K_V + K_R)}{2} \tag{3.3}$$

$$K_V = \frac{(c_{11} + c_{22} + c_{33} + 2(c_{12} + c_{23} + c_{13}))}{9} \tag{3.4}$$

$$K_R = \frac{1}{(s_{11} + s_{22} + s_{33} + 2(s_{12} + s_{22} + s_{13}))} \tag{3.5}$$

$$G_H = \frac{(G_V + G_R)}{2} \tag{3.6}$$

$$G_V = \frac{(c_{11} + c_{22} + c_{33} - (c_{12} + c_{23} + c_{31}) + 3\,(c_{44} + c_{55} + c_{66}))}{15} \tag{3.7}$$

$$G_R = \frac{15}{4\,(s_{11} + s_{22} + s_{33}) - 4\,(s_{12} + s_{23} + s_{31}) + 3\,(s_{44} + s_{55} + s_{66})} \tag{3.8}$$

$$E = \frac{9K_H G_H}{3K_H + G_H} \tag{3.9}$$

where: K_H – approximate mean bulk modulus of Hill method, K_V – approximate upper limit of bulk modulus for Voigt method, K_R – approximate lower limit of bulk modulus for Reuss method, G_H – approximate mean shear modulus of Hill method, G_V – approximate upper limit of shear modulus for Voigt method, G_R – approximate lower limit of shear modulus for Reuss method.

The calculation results calculated by Eq. (3.3)–(3.9) are shown in Table 5.

Table 5. Mechanical properties of three asphalt systems

Types of asphalt	**Elastic modulus (GPa)**	**Bulk modulus (GPa)**	**Shear modulus (GPa)**
Matrix asphalt	0.5684	0.9481	0.2030
Rubber-modified asphalt	0.9171	1.1577	0.3352
Graphene/rubber composite-modified asphalt	0.9297	1.2973	0.3367

As can be seen from Table 5, the mechanical properties of rubber asphalt and graphene/rubber composite-modified asphalt have increased. Compared with the matrix asphalt, the elastic modulus of graphene/rubber composite-modified asphalt increased by 63.56%, the bulk modulus increased by 36.83%, and the shear modulus increased by 65.86%. Obviously, the graphene/rubber composite-modified asphalt greatly improved the mechanical properties of the matrix asphalt, which is related to the swelling development of rubber promoted by graphene, and the rubber formed a stable spatial grid structure in the asphalt. At the same time, graphene is a kind of two-dimensional carbon nanomaterials with high strength and toughness. Under the action of external forces, graphene will dissipate part of the energy generated by external forces, to achieve the purpose of improving the mechanical properties of asphalt.

4. Conclusions

In order to study the modification mechanism of graphene/rubber composite-modified asphalt, the asphalt molecular model, rubber molecular model, and graphene/rubber composite-modified asphalt molecular model were constructed by using molecular dynamics software MS. The modification mechanism was analyzed by the changes of binding energy, radial distribution function, and mechanical properties. The main conclusions are as follows:

1. From the calculation results of binding energy between each component, it is known that the addition of graphene improves the binding energy between rubber and light components in asphalt, indicating that graphene promotes the absorption of rubber to light components, improves the binding stability of rubber and resin, promotes the swelling development of rubber, and improves the compatibility of rubber and asphalt.
2. The results of radial distribution function analysis show that the addition of graphene reduces the aggregation behavior between asphaltene and rubber molecules, and intensifies the aggregation behavior between saturated and aromatic molecules. More light

components in asphalt can penetrate and fill the aggregation space between asphaltenes, improve the overall stability of asphalt system, drive the transformation of asphalt colloid structure, and ultimately improve the high and low temperature performance of asphalt.

3. From the results of mechanical modulus, it is known that graphene promoted the swelling development of rubber, the elastic modulus, bulk modulus and shear modulus of graphene/rubber composite modified asphalt increased by 63.56%, 36.83% and 65.86%, which greatly improved the mechanical properties of asphalt.

Based on the analysis results of the above three parameters, it is feasible to reveal the modification mechanism of graphene/rubber composite-modified asphalt from the atomic scale by using molecular dynamics simulation method, which fully explains how the addition of graphene improves the high and low temperature performance of matrix asphalt, and provides a theoretical basis for the practical application of graphene/rubber composite modified asphalt. Subsequently, building upon the preliminary achievements of the existing research topic, we will further enhance the accuracy of the molecular model, consider a greater variety of asphalt molecules (such as asphaltenes and resins with different molecular weight distributions) and the specific conformations of rubber molecular chains, thereby reflecting the actual material structure more authentically. Concurrently, the modification mechanism research will be continuously deepened to investigate the changes in the molecular dynamic behavior of graphene/rubber composite modified asphalt under different temperatures and aging conditions, including the mobility of molecular chains and the dynamic evolution of interfacial interaction forces. This will enable a more comprehensive and in-depth revelation of the modification mechanism of graphene/rubber composite modified asphalt, optimization of its performance, and promotion of its extensive application in the domain of road engineering.

References

[1] I. Barišić, M. Zvonarić, I. Netinger Grubeša, and S. Šurdonja, "Recycling Waste Rubber Tyres in Road Construction", *Archives of Civil Engineering*, vol. 67, no. 1, pp. 499–512, 2021, doi: 10.24425/ace.2021.136485.

[2] B.Y. Li, "Research on rheological properties of graphene/polyethylene composite modified asphalt binder", *Bulletin of the Chinese Ceramic Society*, vol. 40, pp. 2461–2468, 2021.

[3] J.W. Liu, P.W. Hao, W.T. Jiang, and B.W. Sun, "Rheological properties of SBS modified asphalt incorporated polyvinylpyrrolidone stabilized graphene nanoplatelets", *Construction and Building Materials*, vol. 298, art. no. 123850, 2021, doi: 10.1016/j.conbuildmat.2021.123850.

[4] R.E. Yu, et al., "Polyurethane/graphene oxide nanocomposite and its modified asphalt binder: Preparation, properties and molecular dynamics simulation", *Materials & Design*, vol. 209, art. no. 109994, 2021, doi: 10.1016/j.matdes.2021.109994.

[5] Y.J. Meng, R.J. Zhang, Z.R. Liu, H.Y. Guo, and H.L. Rong, "Research on the influence of graphene on the road performance of rubber powder modified asphalt mixture", *Highway*, vol. 66, pp. 7–11, 2021.

[6] X. Zhang, et al., "Research status of graphene in asphalt composites", *Journal of Central South University (Science and Technology)*, vol. 50, pp. 1637–1644, 2019.

[7] Y.J. Meng, H.Y. Guo, C.C. Xi, H.J. Zhou, and W. Jiang, "Research on high temperature properties of graphene rubber composite modified asphalt", *Journal of Guangxi University (Natural Science Edition)*, vol. 46, pp. 67–73, 2021.

[8] H. Zou and Q. Li, "Research on road performance of graphene compound rubber-modified asphalt and its mixture", *Journal of Highway and Transportation Research and Development*, vol. 37, pp. 46–56, 2020.

[9] H. Yao, Q.L. Dai, Z.P. You, A. Bick, and M. Wang, "Modulus simulation of asphalt binder models using Molecular Dynamics (MD) method", *Construction and Building Materials*, vol. 162, pp. 430–441, 2018, doi: 10.1016/j.conbuildmat.2017.09.106.

[10] Z.X. Chen, J.Z. Pei, R. Li, and F.P. Xiao, "Performance characteristics of asphalt materials based on molecular dynamics simulation-A review", *Construction and Building Materials*, vol. 189, pp. 695–710, 2018, doi: 10.1016/j.conbuildmat.2018.09.038.

[11] C.H. Yu, et al., "Analysis of the Storage Stability Property of Carbon Nanotube/Recycled Polyethylene-Modified Asphalt Using Molecular Dynamics Simulations", *Polymers*, vol. 13, no. 10, art. no. 1658, 2021, doi: 10.3390/polym13101658.

[12] X. Qu, D.W. Wang, L.B. Wang, Y.C. Huang, Y. Hou, and M. Oeser, "The State-of-the-Art Review on Molecular Dynamics Simulation of Asphalt Binder", *Advances in Civil Engineering*, vol. 2018, art. no. 4546191, 2018, doi: 10.1155/2018/4546191.

[13] J.Z. Liu, Q. Liu, S.Y. Wang, X.Y. Zhang, C.Y. Xiao, and X.B. Yu, "Molecular dynamics evaluation of activation mechanism of rejuvenator in reclaimed asphalt pavement (RAP) binder", *Construction and Building Materials*, vol. 298, art. no. 123898, 2021, doi: 10.1016/j.conbuildmat.2021.123898.

[14] W. Sun and H. Wang, "Moisture effect on nanostructure and adhesion energy of asphalt on aggregate surface: A molecular dynamics study", *Applied Surface Science*, vol. 510, art. no. 145435, 2020, doi: 10.1016/j.apsusc.2020.145435.

[15] Y. Kang, et al., "Molecular dynamics study on the glass forming process of asphalt", *Construction and Building Materials*, vol. 214, pp. 430–440, 2019, doi: 10.1016/j.conbuildmat.2019.04.138.

[16] J.L. Pan, M. Hossain, and R. Tarefder, "Combined effects of oxidative aging and moisture inclusion on asphalt binder using Molecular Dynamic simulation", in *Asphalt Pavements*. CRC Press, 2014, pp. 1785–1794.

[17] Y.L. Yaphary, Z. Leng, H.P. Wang, S.S. Ren, and G.Y. Lu, "Characterization of nanoscale cracking at the interface between virgin and aged asphalt binders based on molecular dynamics simulations", *Construction and Building Materials*, vol. 335, art. no. 127475, 2022, doi: 10.1016/j.conbuildmat.2022.127475.

[18] M. Zadshir, D.J. Oldham, S. Hosseinnezhad, and E.H. Fini, "Investigating bio-rejuvenation mechanisms in asphalt binder via laboratory experiments and molecular dynamics simulation", *Construction and Building Materials*, vol. 190, pp. 392–402, 2018, doi: 10.1016/j.conbuildmat.2018.09.137.

[19] G.J. Xu and H. Wang, "Molecular dynamics study of interfacial mechanical behavior between asphalt binder and mineral aggregate", *Construction and Building Materials*, vol. 121, pp. 246–254, 2016, doi: 10.1016/j.conbuildmat.2016.05.167.

[20] F.H. Nie, W. Jian, and D. Lau, "An atomistic study on the thermomechanical properties of graphene and functionalized graphene sheets modified asphalt", *Carbon*, vol. 182, pp. 615–627, 2021, doi: 10.1016/j.carbon.2021.06.055.

[21] D.D. Li and M.L. Greenfield, "Chemical compositions of improved model asphalt systems for molecular simulations", *Fuel*, vol. 115, pp. 347–356, 2014, doi: 10.1016/j.fuel.2013.07.012.

[22] L.Q. Zhang and M.L. Greenfield, "Analyzing properties of model asphalts using molecular simulation", *Energy & Fuels*, vol. 21, no. 3, pp. 1712–1716, 2007, doi: 10.1021/ef060658j.

[23] K. Hu, C.H. Yu, Y.J. Chen, W. Li, D.D. Wang, and W.G. Zhang, "Multiscale mechanisms of asphalt performance enhancement by crumbed waste tire rubber: insight from molecular dynamics simulation", *Journal of Molecular Modeling*, vol. 27, art. no. 170, 2021, doi: 10.1007/s00894-021-04786-1.

[24] X.X. Zhou, X. Zhang, S. Xu, S.P. Wu, G.T. Liu, and Z.P. Fan, "Evaluation of thermo-mechanical properties of graphene/carbon-nanotubes modified asphalt with molecular simulation", *Molecular Simulation*, vol. 43, no. 4, pp. 312–319, 2017, doi: 10.1080/08927022.2016.1274985.

[25] X.F. Jia, "Study on performance of crumb rubber / SBS composite modified asphalt and mixture", M.A. thesis, Lanzhou Jiaotong University, Lanzhou, 2020.

[26] L. Yang, "Molecular dynamics simulation and rheological properties of graphene modified asphalt binders", M.A. thesis, Northwest A&F University, Xi'an, 2021.

[27] X.Y. Zhu, Z. Du, H.W. Ling, L. Chen, and Y.H. Wang, "Effect of filler on thermodynamic and mechanical behavior of asphalt mastic: a MD simulation study", *International Journal of Pavement Engineering*, vol. 21, no. 10, pp. 1248–1262, 2020, doi: 10.1080/10298436.2018.1535120.

[28] L.X. Huang, K. Zhou, and J. Huang, "Molecular dynamics simulation of temperature effect on interface microstructure of graphene/asphalt composites", *Highway*, vol. 67, pp. 349–356, 2022.

[29] A.M. Adnan and J.C. Wang, "Enhancement of rheological performance and compatibility of tire rubber-modified asphalt binder with the addition of graphene", *Construction and Building Materials*, vol. 402, art. no. 133038, 2023, doi: 10.1016/j.conbuildmat.2023.133038.

[30] H.Q. He, P.F. Gou, R. Li, J.Z. Pei, B.W. Xie, and K. Yang, "Optimum preparation and rheological properties of liquid rubber-modified asphalt binder", *Construction and Building Materials*, vol. 347, art. no. 128551, 2022, doi: 10.1016/j.conbuildmat.2022.128551.

[31] L. Chu, L. Luo, and T.F. Fwa, "Effects of aggregate mineral surface anisotropy on asphalt-aggregate interfacial bonding using molecular dynamics (MD) simulation", *Construction and Building Materials*, vol. 225, pp. 1–12, 2019, doi: 10.1016/j.conbuildmat.2019.07.178.

[32] Y.J. Meng, H.Y. Guo, R.G. Xu, R.J. Zhang, and C.X. Ma, "Rheological and microscopic properties of graphene rubber composite modified asphalt", *Journal of Building Materials*, vol. 23, pp. 1246–1251, 2020.

[33] B.M. Tang, Y.J. Ding, H.Z. Zhu, and X.J. Cao, "Study on the change characteristics of asphalt molecular aggregation state", *China Journal of Highway and Transport*, vol. 26, pp. 50–56+76, 2013.

[34] F.C. Guo, J.P. Zhang, J.Z. Pei, B.C. Zhou, and Z. Hu, "Study on the mechanical properties of rubber asphalt by molecular dynamics simulation", *Journal of Molecular Modeling*, vol. 25, no. 12, art. no. 365, 2019, doi: 10.1007/s00894-019-4250-x.

[35] H.N. Yu, J.G. Ge, G.P. Qian, C. Zhang, W. Dai, and P. Li, "Evaluation on the rejuvenation and diffusion characteristics of waste cooking oil on aged SBS asphalt based on molecular dynamics method", *Journal of Cleaner Production*, vol. 406, art. no. 136998, 2023, doi: 10.1016/j.jclepro.2023.136998.

Received: 2024-04-24, Revised: 2024-10-16